

# Effects of sample geometry and draw conditions on the mechanical properties of drawn poly(ethylene terephthalate)

Masayoshi Ito\*, Katsumi Takahashi and Tetsuo Kanamoto†

Departments of Chemistry and †Applied Chemistry, Science University of Tokyo, Kagurazaka, Shinjuku-ku, Tokyo 162, Japan

(Received 30 December 1988; revised 9 February 1989; accepted 11 March 1989)

Fibres and films prepared from solutions of high molecular weight poly(ethylene terephthalate) were drawn by two-stage drawing, tensile drawing or co-extrusion at low temperature (25–80°C) followed by tensile drawing at high temperature (230°C). Both fibres and films could be drawn up to a draw ratio of 11 by this method. The mechanical properties of drawn samples were greatly affected by the draw temperature for the first stage and the tension applied to the samples during cooling after the second-stage. The highest tensile modulus and strength for the drawn fibres that could be attained were 29.5 and 1.4 GPa, respectively, at the highest draw ratio of 11. For the films, the corresponding values were about half of those achieved for the fibres. The remarkable difference is closely related to the difference in amorphous chain orientation between drawn fibres and films, reflecting the different processing conditions available for each sample, and cross-sectional area.

(Keywords: poly(ethylene terephthalate); solution-spun fibre; cast film; sample geometry; draw conditions; mechanical properties; superstructure)

## INTRODUCTION

Much effort has been expended to increase the mechanical properties of drawn poly(ethylene terephthalate) (PET) fibres and films. Kunugi *et al.*<sup>1,2</sup> and Amano and Nakagawa<sup>3</sup> developed a new route to high modulus materials by zone annealing and microwave heat drawing techniques, respectively. However, the moduli reported in their literatures are only 14–23% of the crystal modulus of PET along the molecular chain, 107.8 GPa (Reference 4). Ito *et al.* have shown<sup>5</sup> that the initial morphology and molecular weight of PET have a remarkable effect on the deformability and tensile properties of the resultant drawn materials. At a given deformation ratio, the tensile strength of drawn films increased with increasing molecular weight. It was also reported<sup>1,2</sup> that the mechanical properties of drawn fibres were higher than those of drawn films although both samples were prepared by the same technique.

In this study films and fibres prepared from solutions of high molecular weight PET chips were drawn by two-stage drawing, tensile drawing or co-extrusion at low temperature followed by conventional tensile drawing at high temperature. The results are discussed in terms of the effects of sample geometry and draw conditions on the resultant mechanical properties of drawn PET.

## EXPERIMENTAL

PET chips with intrinsic viscosity  $1.76 \text{ dl g}^{-1}$  were supplied by Toyobo Co. The films were produced from a 15 wt% polymer solution prepared under nitrogen atmosphere by dissolving the dry chips at 205°C in

nitrobenzene. The concentration was a maximum for the polymer–solvent system used. Solution cast (SC) films were produced by casting the polymer solution on a glass plate that had been precooled at 5–6°C.

For the preparation of fibres, extrusion of the 15 wt% polymer solution was examined at 195°C through a conical capillary die with a diameter of 0.2 mm. However, spinning was difficult due to the low viscosity of the polymer solution. Fibres could be obtained by extrusion of the wet SC films at 195°C through the capillary die. The polymer concentration in the wet SC film was adjusted to 50 wt% by removing the solvent at 80°C under vacuum. At the extrusion temperature of 195°C, the wet films changed into a wet gel and/or a polymer solution. The wet gel and/or the polymer solution transformed into wet fibres immediately after coming out from the die at room temperature. The wet fibres were collected on a glass bobbin under tension free conditions. Most of the solvent (>90 wt%) in the films and as-spun fibres was removed at room temperature under vacuum.

A two-stage drawing technique was used. For the first stage, a solid-state coextrusion technique<sup>6</sup> or conventional tensile drawing was used. The SC films or as-spun fibres were placed between two split-billet halves of commercial polyethylene, and the assembly was coextruded at 80°C. Tensile drawing was done at room temperature. For the second stage draw, the conventional tensile drawing was done at 230°C. After the second stage draw, all the drawn samples were cooled to room temperature under constant tension. No residual solvent was recognized in the infrared (i.r.) spectra of drawn fibres and films after the second stage draw. The total draw ratio (TDR) was determined by measuring the separation between lateral ink marks on the sample before and after drawing.

\* To whom correspondence should be addressed

### Measurements

The tensile modulus and strength of drawn films and fibres along the fibre axis were measured at room temperature at a strain rate of  $1 \times 10^{-3} \text{ s}^{-1}$  and  $1 \times 10^{-2} \text{ s}^{-1}$ , respectively. The modulus was determined from the slope of the stress-strain curve at low strain ( $<0.1\%$ ). The birefringence was measured by a polarizing microscope equipped with a Berek compensator and quartz plate as an additional compensator. Weight percentage crystallinity was calculated from the sample density, which was obtained at  $30^\circ\text{C}$  in a density gradient column using n-heptane and carbon tetrachloride. The amorphous and crystalline densities for PET were taken to be  $1.333$  and  $1.455 \text{ g cm}^{-3}$ , respectively<sup>7</sup>.

## RESULTS AND DISCUSSION

### Drawing behaviour of as-spun fibres and cast films

The mechanical properties of the drawn samples were greatly affected by the cross sectional area (CSA) of the samples. The CSA of as-spun fibres was chosen to be in the range  $1.8 \times 10^{-4}$ – $3.1 \times 10^{-4} \text{ cm}^2$  by controlling the spinning speed. The SC films of thickness  $100 \mu\text{m}$  were cut into narrow strips to adjust the CSA in the range  $1.8 \times 10^{-3}$ – $22 \times 10^{-3} \text{ cm}^2$ .

Wide angle X-ray diffraction patterns of all the samples revealed that less perfect crystals were developed with no selective chain orientation. The crystallinities of as-spun fibres and SC films evaluated from observed densities were  $\approx 27$  and  $\approx 55\%$ , respectively.

As-spun fibres could be drawn to a draw ratio of 4–5 at room temperature (first stage draw). These fibres were further drawn by a tensile tester at a constant temperature of  $170$ – $250^\circ\text{C}$  (second stage draw). At the second stage draw, the attainable total draw ratio ( $\text{TDR}_{\text{max}}$ ) increased slightly with draw temperature from 8 at  $170^\circ\text{C}$  to 11.5 at  $230^\circ\text{C}$ . For drawing above  $240^\circ\text{C}$ , both  $\text{TDR}_{\text{max}}$  and the tensile strength of the resultant drawn fibres decreased with increasing temperature. So, the second stage draw for all the samples was done at  $230^\circ\text{C}$ . Single stage tensile drawing was also examined at this temperature. However, both the achievable draw ratio and the mechanical properties of the resultant drawn fibres were low compared with those for fibres produced by the two stage draw. The main effect of the first stage draw at low temperature on the fibre properties is discussed in the next section.

The SC films were brittle due to high crystallinity and they could not be drawn at room temperature. It is well known that unoriented semicrystalline PET is not readily cold drawn by tensile force since crystals act as stress concentrators and thereby lead to a failure. However, Pereira and Porter<sup>8</sup> have shown that semicrystalline PET (50% crystallinity) can be effectively drawn by using a solid-state coextrusion technique. They report that the technique involves deformation under pressure on a double substrate, which minimizes the stress concentration and enhances the crystal destruction. In this work solid-state coextrusion was used for the first stage drawing of the SC films. By this method, the cast films could be drawn to a draw ratio of 5 at  $80^\circ\text{C}$ . The as-spun fibres were also coextruded at  $80^\circ\text{C}$  for comparison. These extrudates were further drawn at  $230^\circ\text{C}$  by a conventional tensile drawing technique.  $\text{TDR}_{\text{max}}$  was  $\approx 11$  for the SC films and fibres. In this study, three series of drawn samples were prepared.

(A) drawn fibres prepared by tensile drawing at room temperature followed by tensile drawing at  $230^\circ\text{C}$ ;

(B) drawn fibres prepared by coextrusion at  $80^\circ\text{C}$  followed by tensile drawing at  $230^\circ\text{C}$ ; and

(C) drawn films prepared by coextrusion at  $80^\circ\text{C}$  followed by tensile drawing at  $230^\circ\text{C}$ .

### Relation between sample size and mechanical properties

The tensile modulus and strength of drawn samples were complexly affected by several factors including TDR, sample geometry, draw temperature at the first stage and the tension applied to the sample during cooling from the drawing temperature ( $230^\circ\text{C}$ ) to room temperature. It has been reported<sup>9</sup> that the apparent tensile modulus of highly drawn polyethylene, at a given draw ratio, is highly dependent on the aspect ratio (ratio of sample length and lateral size). Figure 1 shows the dependence of tensile modulus on aspect ratio for three samples with a draw ratio of 8.5 which were prepared under the highest tension applicable to the samples. In this figure, the aspect ratio was varied by changing the length of the sample with a constant CSA. Clearly, the apparent modulus increases with increasing aspect ratio, with saturation at  $\approx 100$  and  $\approx 1000$  for the films and the fibres, respectively. It is assumed<sup>10</sup> that the non-uniform stress distribution, which arises from the particular method used to transfer an external force to oriented samples, becomes uniform at a distance away from the points of application. The distance is  $d = b(E/G)^{1/2}$ , where  $b$  is the maximum lateral dimension of the sample,  $E$  is Young's modulus along the axis of the sample and  $G$  the longitudinal shear modulus. In this case, stress concentrations imposed at the ends of the sample can be neglected in the calculation of the elastic constants. The value of  $G$  for oriented PET film might be  $\approx 0.7 \text{ GPa}$  (Reference 11). The tensile modulus for the present samples is  $\approx 20 \text{ GPa}$ . If one takes these values, then  $(E/G)^{1/2} \approx 5$ , suggesting that the end effect should start to decrease for an aspect ratio of 12, which disagrees with the experimental results. For the present samples, the lateral dimension of drawn films is about 10 times that of drawn fibres. This means that drawn films with an aspect ratio of 100 have a similar sample length to drawn fibres with an aspect ratio of 1000. When the modulus data in Figure 1 were plotted as a function of

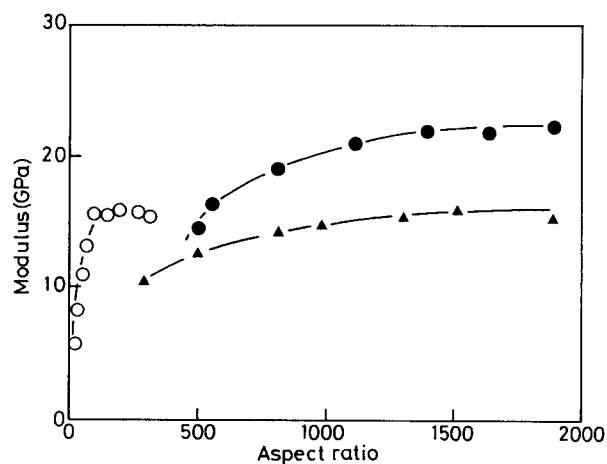


Figure 1 Tensile modulus versus aspect ratio for: ●, series A; ▲, series B; and, ○, series C.  $\text{TDR} = 8.5$

real sample length (data not shown), a plateau was reached at a sample length of  $\approx 10$  cm for the three series.

From these results the following points are emphasized. A long sample length is required before the maximum plateau value is reached on the modulus-sample length curve. The length required is longer than the value estimated from Horgan's equation<sup>10</sup> and is independent of the shape and the area of cross section. Thus the sample length was chosen to be 10 cm in the following tensile tests. Although a large discrepancy exists between the present results and the prediction of Horgan<sup>10</sup>, the problem is not our concern here.

In Figure 2, tensile moduli are plotted against the tension applied to the samples during cooling from 230°C to room temperature for the samples with a TDR of 9.5. The modulus increases gradually with increasing tension. A high tension might exert a considerable constraint on the mobility of oriented non-crystalline molecules and thus restrict their relaxation during cooling. It is also seen that the maximum tension applicable to the samples is higher for series A than for series B and C, although samples from both series A and B were prepared from the as-spun fibres with a similar CSA. Further, at a given tension, the moduli of samples of series A are higher than those of series B and C. As mentioned above, the drawing conditions for the first stage for series A are different from those for series B and C. These results clearly indicate that the draw conditions for the first stage draw have a major effect on the superstructure of two stage drawn samples, which will be discussed later. The maximum tension applicable to the samples also depends on the cross-sectional area of the samples, as seen in Figure 3 in which tension is plotted against cross-sectional area of samples of series A drawn to a TDR of 10. The tension increases with decreasing cross-sectional area. The relation is closely related to the tensile strength of the samples, as will be shown later.

The tensile modulus is also dependent on the draw ratio of the samples. In Figure 4, tensile modulus is plotted against TDR. As mentioned above, the modulus is affected by the tension (Figure 2). Thus the plots in Figure 4 were carried out for the samples prepared under the highest tension applicable at each TDR. For series A, the modulus increases almost linearly with increasing TDR, and the maximum modulus achieved is 29.5 GPa for the sample with the highest TDR of 11.5. At a given TDR, the moduli for series B and C are lower than those for series A. The achievable maximum modulus for series B and C is about half of that for series A, although the

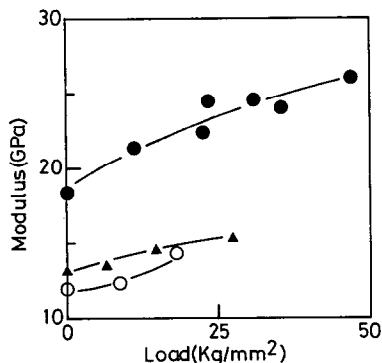


Figure 2 Tensile modulus versus load for: ●, series A; ▲, series B; and, ○, series C. TDR=9.5

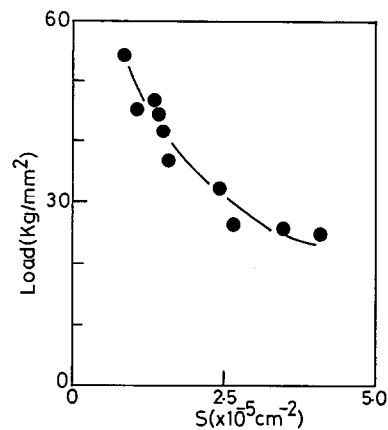


Figure 3 Maximum load applicable to the samples versus cross-sectional area for series A at TDR = 10

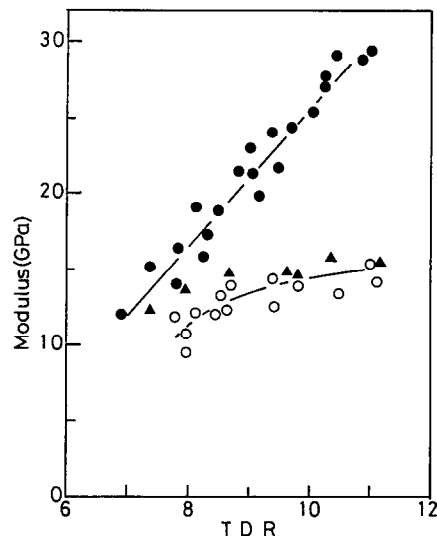


Figure 4 Tensile modulus versus TDR for: ●, series A; ▲, series B; and, ○, series C

highest TDR for the former is comparable with that for the latter. This is again due to the difference in the draw condition used for the first-stage draw. Itoyama<sup>12</sup> studied the effects of prolonged annealing on the structure and properties of drawn PET fibres and reported that the dynamic modulus of the fibre increased appreciably with treatment time at 260°C from 18.9 GPa at 24 h to 35.4 GPa at 360 h. Note that, in the present study, the high modulus of 29.5 GPa could be achieved by two stage drawing without any additional heat treatments of drawn samples. Previous work<sup>13</sup> on the drawing of acetone treated PET fibres revealed that prolonged heat treatments at high temperatures improved the tensile modulus but caused molecular degradation, which resulted in a marked decrease in the tensile strength of the samples.

In Figure 5, the tensile strengths of drawn samples with a TDR of 9.5 are plotted against the tension applied to the samples during cooling from 230°C to room temperature. Similarly to the case of modulus versus tension, the strength increases significantly with increasing tension. At a given tension, the strength of series B is lower than that of series A despite the fact that both samples were prepared from the as-spun fibres with a similar CSA under the same conditions. Further, the maximum tension applicable to series B is lower than

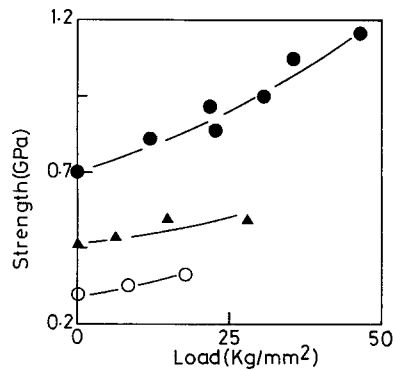


Figure 5 Tensile strength versus load for: ●, series A; ▲, series B; and, ○, series C. TDR=9.5

that applicable to series A (see Figures 2 and 5). These results are closely related to the efficiency of draw achieved at the first stage draw.

As shown in Figure 3, the maximum tension applicable to the samples increased with decreasing cross-sectional area. Thus, the smaller the cross-sectional area, the higher was the tensile modulus and strength that could be achieved. In general, the fibre strength is related to the microstructure and the presence of impurities, defects and surface flaws<sup>14</sup>. Pennings *et al.*<sup>15</sup> proposed a relation between tensile strength and fibre diameter according to the concept of surface flaw<sup>16</sup>, where cracks are assumed to be initiated:

$$\sigma_b^{-1} = K(D - D_0)^{1/2} + \sigma_0^{-1} \quad (1)$$

where  $\sigma_b$  and  $\sigma_0$  are the tensile strengths of the measured and flawless fibres, respectively,  $D$  and  $D_0$  are the diameters of measured and flawless fibres, respectively, and  $K$  is a constant. The applicability of equation (1) to the drawn fibres (series A) with a TDR of 10 is examined in Figure 6. The samples were prepared under a constant tension of  $40 \text{ kg mm}^{-2}$ . It is evident that a linear relationship is not found between  $\sigma_b^{-1}$  and  $D^{1/2}$  although  $\sigma_b^{-1}$  increases with increasing  $D^{1/2}$ . This fact implies that the strength of these drawn PET samples is not directly related to surface flaws but depends on other factors including the microstructure.

The tensile strength is also a function of the TDR of the samples. In Figure 7, tensile strength is plotted as a function of TDR for the samples of the three series prepared under the highest tension applicable. With increasing TDR, the strength increases, with this tendency most prominent for series A. The highest value of 1.4 GPa was achieved for series A at the highest TDR of 11.5. At a given TDR, a large difference in strength is observed among the three series. This is due to the difference in the cross-sectional area of the samples and in the superstructure which was produced under different draw temperatures at the first stage draw and to different tensions applied to the samples during cooling after the second-stage draw.

#### Superstructure

Figure 8 shows the TDR dependence of the chain orientation factors of crystalline ( $F_c$ ) and amorphous ( $F_a$ ) regions of samples which were prepared under the highest tension applicable.  $F_c$  was evaluated by the well known X-ray diffraction method<sup>17</sup>.  $F_a$  was evaluated by combining optical birefringence data with  $F_c$  and sample

crystallinity data. The intrinsic birefringences of the crystal and the amorphous phases were taken to be 0.251 and 0.230, respectively<sup>1</sup>. The results demonstrate that the  $F_c$  for all the samples are close to each other, and stay at an almost constant value of 0.94 for TDR > 8. On the other hand, the  $F_a$  are dependent on the sample history

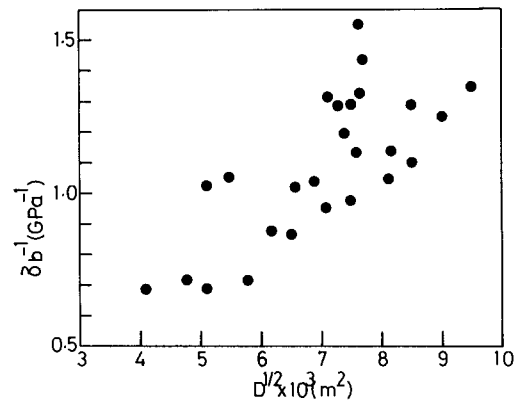


Figure 6 Relation between tensile strength and fibre diameter for series A at TDR = 10

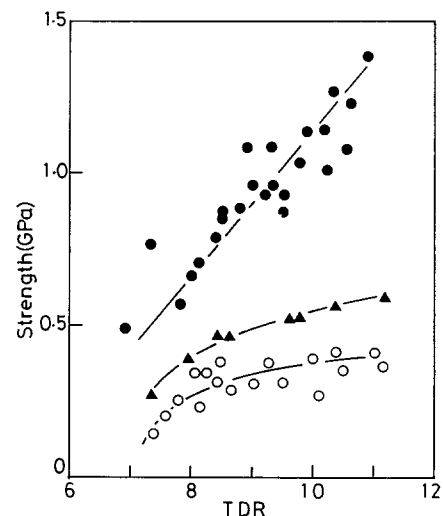


Figure 7 Tensile strength versus TDR for: ●, series A; ▲, series B; and, ○, series C

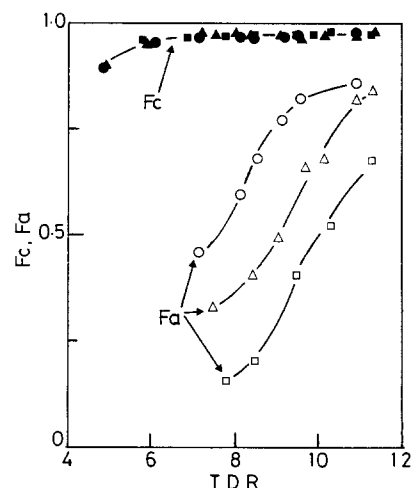


Figure 8 Chain orientation factors in crystalline ( $F_c$ ) and amorphous ( $F_a$ ) regions versus TDR for: ●, ○, series A; ▲, △, series B; and, ■, □, series C

and the TDR. With increasing TDR,  $F_a$  increases for each series. Further, at a given TDR, series A shows the highest value among the three series. In Figure 9, thermal shrinkage of the samples with a TDR of 11 is plotted against measurement temperature. All the samples show a large shrinkage around 80–100°C, with this tendency more prominent for series B and C. The large shrinkage is due to the rubber elastic contraction of the amorphous regions<sup>18</sup>. Note that the sample with the highest  $F_a$  value (series A) shows the lowest shrinkage among the three series. This indicates that a simple series combination of crystalline and non-crystalline regions cannot be considered as the structural model for the present drawn samples. In Figure 10, sample densities and crystallinities are plotted against TDR. At the first stage draw (TDR < 5), the density decreases with increasing TDR due to the partial destruction of the crystals<sup>8</sup>. At the second stage draw (TDR > 5), the density increases remarkably, with this effect most prominent for series A. During the second stage draw at 230°C, a large amount of crystals is formed with increased chain alignment in the crystalline regions (Figure 8). Note that the sample with the highest amorphous orientation shows the largest increase in density and hence apparently in crystallinity. This suggests that some of the taut tie molecules are

incorporated into crystallites and form the crystalline bridges during the second stage draw. Although the crystalline bridges are suggested to be a necessary structure to produce high modulus and high strength materials, present thermal shrinkage and mechanical data imply that such structures are not well developed even in series A.

As mentioned above, the tensile strength at a given TDR increased with increasing tension applied to the samples during cooling from 230°C to room temperature. Further, the maximum tension applicable to the sample was dependent on the conditions used for the first stage draw. The tensile strengths of the first-stage drawn samples at a draw ratio of 3.5 were 340, 180 and 110 MPa, for series A, B and C, respectively. The higher strength for series A can be attributed to the fact that, as a result of drawing below  $T_g$ , the strained tie molecules produced are larger in number and more constrained. Such a superstructure is probably enhanced during the second stage drawing and makes it possible to apply a high tension to the samples after the second stage draw at high temperature. Under the higher tension, the relaxation of strained tie molecules is severely restricted, resulting in the production of high modulus and high strength PET fibres and films.

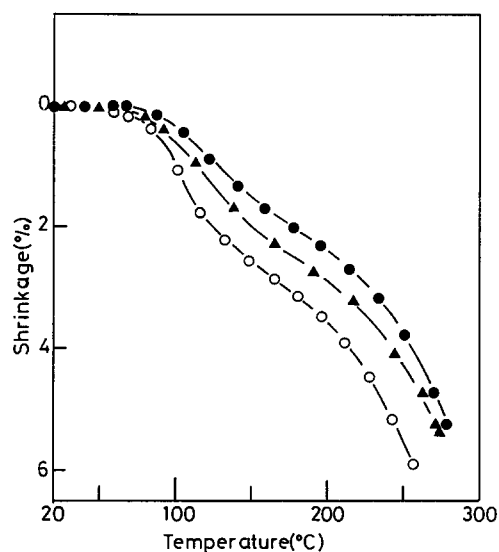


Figure 9 Thermal shrinkage versus temperature for: ●, series A; ▲, series B; and, ○, series C. TDR = 11

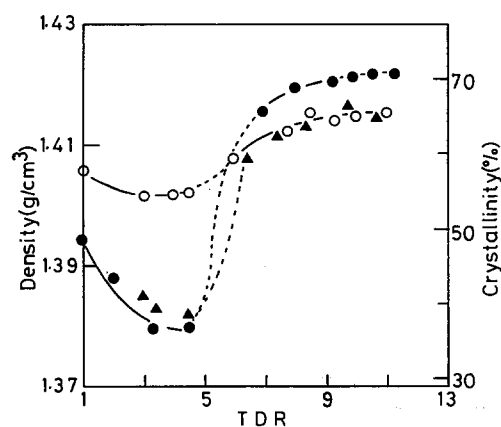


Figure 10 Density and crystallinity versus TDR for: ●, series A; ▲, series B; and, ○, series C

## CONCLUSIONS

Films and fibres from high molecular weight PET chips could be drawn up to a draw ratio of 11 by two stage drawing. The draw conditions used for the first stage draw, the tension applied to the samples during cooling after the second stage draw and the cross-sectional area of the samples have a marked effect on the tensile properties of the resultant drawn samples. These are closely related to the degree of orientation in the non-crystalline regions. The lower the draw temperature at the first-stage draw and the smaller the cross-sectional area of the samples, the higher is the tension that can be applied to the samples, which leads to the high orientation in the amorphous chains and results in the high modulus and high strength drawn PET samples. Under the optimum draw condition, the tensile modulus and strength for the drawn fibres reached 29.5 and 1.4 GPa, respectively. These values are about twice those for drawn films. The crystallinity of drawn PET is not as high as for highly drawn polyethylene. In this case, the enhancement of amorphous chain orientation is probably the major factor in achieving high modulus and high strength drawn PET.

## REFERENCES

- 1 Kunugi, T., Suzuki, A. and Hashimoto, M. *J. Appl. Polym. Sci.* 1981, **26**, 1951
- 2 Kunugi, T., Ichinose, C. and Suzuki, A. *J. Appl. Polym. Sci.* 1986, **31**, 429
- 3 Amano, M. and Nakagawa, K. *Polymer* 1986, **27**, 1559
- 4 Sakurada, I. and Kaji, K. *Kobunshi Kagaku* 1969, **26**, 817
- 5 Ito, M., Tanaka, K. and Kanamoto, T. *J. Polym. Sci., Polym. Phys. Edn* 1987, **25**, 2127
- 6 Griswold, P. D., Zachariades, A. E. and Porter, R. S. *Polym. Eng. Sci.* 1976, **18**, 861
- 7 Duibeny, R. De P., Bun, C. W. and Brown, C. J. *Proc. R. Soc. Lond.* 1955, **A226**, 531
- 8 Pereira, J. R. C. and Porter, R. S. *J. Polym. Sci., Polym. Phys. Edn* 1983, **21**, 1147
- 9 Arridge, R. G. C. and Folks, M. J. *Polymer* 1976, **17**, 495
- 10 Horgan, C. O. *Int. J. Solids Struct.* 1974, **10**, 837

- 11 Ward, I. M. *J. Macromol. Sci.* 1967, **B1**, 667
- 12 Itoyama, K. *J. Polym. Sci., Polym. Lett.* 1987, **25**, 331
- 13 Ito, M., Miya, H., Kanamoto, T. and Tanaka, K. *Rep. Progr. Polym. Phys. Jpn* 1988, **31**, 313
- 14 Magat, E. E. *Phil. Trans. R. Soc. Lond.* 1980, **A294**, 463
- 15 Pennings, A. J., Smook, J., de Boer, J., Gogolewski, S. and van Hutten, P. F. *Pure Appl. Chem.* 1983, **55**, 777
- 16 Griffith, A. A. *Phil. Trans. R. Soc. Lond.* 1921, **A221**, 163
- 17 Gupta, V. B., Ramesh, C., Patil, N. B. and Chidambareswaran, P. K. *J. Polym. Sci., Polym. Phys. Edn* 1983, **21**, 2425
- 18 Choy, C. L., Chen, F. C. and Yong, K. *J. Polym. Sci., Polym. Phys. Edn* 1981, **19**, 335